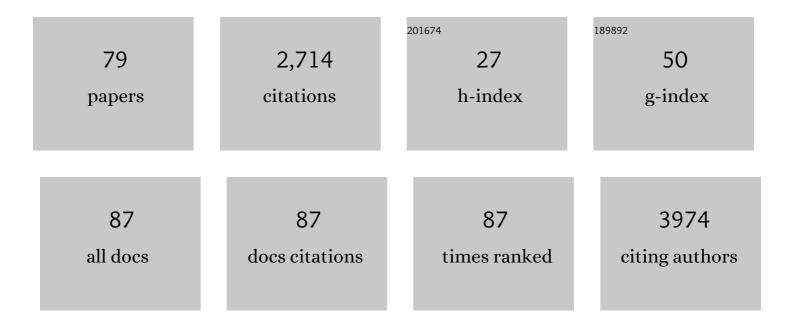
Tae-Young Yoon

List of Publications by Year in descending order

Source: https://exaly.com/author-pdf/4877745/publications.pdf Version: 2024-02-01



#	Article	lF	CITATIONS
1	Untangling the complexity of membrane protein folding. Current Opinion in Structural Biology, 2022, 72, 237-247.	5.7	11
2	Emerging Biophysics Tools for Biologists. Molecules and Cells, 2022, 45, 4-5.	2.6	0
3	Structural basis of neuropeptide Y signaling through Y1 receptor. Nature Communications, 2022, 13, 853.	12.8	20
4	High-Resolution Single-Molecule Magnetic Tweezers. Annual Review of Biochemistry, 2022, 91, 33-59.	11.1	25
5	Evolutionary balance between foldability and functionality of a glucose transporter. Nature Chemical Biology, 2022, 18, 713-723.	8.0	13
6	Encoding Multiple Virtual Signals in DNA Barcodes with Single-Molecule FRET. Nano Letters, 2021, 21, 1694-1701.	9.1	12
7	Extreme parsimony in ATP consumption by 20S complexes in the global disassembly of single SNARE complexes. Nature Communications, 2021, 12, 3206.	12.8	8
8	Simultaneous Real-Time Three-Dimensional Localization and FRET Measurement of Two Distinct Particles. Nano Letters, 2021, 21, 7479-7485.	9.1	4
9	Single-molecule functional anatomy of endogenous HER2-HER3 heterodimers. ELife, 2020, 9, .	6.0	14
10	Studying the Effects of Inositol Pyrophosphates in an In Vitro Vesicle–Vesicle Fusion Assay. Methods in Molecular Biology, 2020, 2091, 145-152.	0.9	0
11	The HER2 S310F Mutant Can Form an Active Heterodimer with the EGFR, Which Can Be Inhibited by Cetuximab but Not by Trastuzumab as well as Pertuzumab. Biomolecules, 2019, 9, 629.	4.0	10
12	Shedding light on complexity of protein–protein interactions in cancer. Current Opinion in Chemical Biology, 2019, 53, 75-81.	6.1	7
13	Synaptic vesicle fusion: today and beyond. Nature Structural and Molecular Biology, 2019, 26, 663-668.	8.2	23
14	Submicrometer elasticity of double-stranded DNA revealed by precision force-extension measurements with magnetic tweezers. Science Advances, 2019, 5, eaav1697.	10.3	50
15	Profiling protein–protein interactions of single cancer cells with in situ lysis and co-immunoprecipitation. Lab on A Chip, 2019, 19, 1922-1928.	6.0	14
16	Watching helical membrane proteins fold reveals a common N-to-C-terminal folding pathway. Science, 2019, 366, 1150-1156.	12.6	59
17	Phosphorylated EGFR Dimers Are Not Sufficient to Activate Ras. Cell Reports, 2018, 22, 2593-2600.	6.4	62
18	SNARE complex assembly and disassembly. Current Biology, 2018, 28, R397-R401.	3.9	116

#	Article	IF	CITATIONS
19	Profiling of protein–protein interactions via single-molecule techniques predicts the dependence of cancers on growth-factor receptors. Nature Biomedical Engineering, 2018, 2, 239-253.	22.5	18
20	Singleâ€Molecule Coâ€Immunoprecipitation Reveals Functional Inheritance of EGFRs in Extracellular Vesicles. Small, 2018, 14, e1802358.	10.0	12
21	Focused clamping of a single neuronal SNARE complex by complexin under high mechanical tension. Nature Communications, 2018, 9, 3639.	12.8	15
22	Reconstruction of LPS Transfer Cascade Reveals Structural Determinants within LBP, CD14, and TLR4-MD2 for Efficient LPS Recognition and Transfer. Immunity, 2017, 46, 38-50.	14.3	274
23	Review: Progresses in understanding Nâ€ethylmaleimide sensitive factor (NSF) mediated disassembly of SNARE complexes. Biopolymers, 2016, 105, 518-531.	2.4	48
24	Inositol pyrophosphates inhibit synaptotagmin-dependent exocytosis. Proceedings of the National Academy of Sciences of the United States of America, 2016, 113, 8314-8319.	7.1	41
25	Observing Extremely Weak Protein–Protein Interactions with Conventional Single-Molecule Fluorescence Microscopy. Journal of the American Chemical Society, 2016, 138, 14238-14241.	13.7	21
26	PIF1-Interacting Transcription Factors and Their Binding Sequence Elements Determine the in Vivo Targeting Sites of PIF1. Plant Cell, 2016, 28, 1388-1405.	6.6	68
27	Seeing an explosive way of NSF/SNAP-mediated SNARE-complex disassembly using single-molecule measurements. , 2015, , .		0
28	Spring-loaded unraveling of a single SNARE complex by NSF in one round of ATP turnover. Science, 2015, 347, 1485-1489.	12.6	73
29	Mapping the energy landscape for second-stage folding of a single membrane protein. Nature Chemical Biology, 2015, 11, 981-987.	8.0	78
30	Microfluidic Synthesis of Hybrid Nanoparticles with Controlled Lipid Layers: Understanding Flexibility-Regulated Cell–Nanoparticle Interaction. ACS Nano, 2015, 9, 9912-9921.	14.6	163
31	Programmed folding of DNA origami structures through single-molecule force control. Nature Communications, 2014, 5, 5654.	12.8	43
32	New Antifouling Platform Characterized by Single-Molecule Imaging. ACS Applied Materials & Interfaces, 2014, 6, 3553-3558.	8.0	21
33	Single Molecule Force Control Drives the Rapid Assembly of DNA Nanostructure. Biophysical Journal, 2014, 106, 279a.	0.5	0
34	Single-Cell Single-Molecule Co-IP Analysis. Biophysical Journal, 2014, 106, 196a-197a.	0.5	0
35	Single Molecule Diagnostic Method to Reveal Cancer-Related EGFR Signaling. Biophysical Journal, 2014, 106, 224a.	0.5	0
36	Real-Time Observation of Multiple-Protein Complex Formation with Single-Molecule FRET. Journal of the American Chemical Society, 2013, 135, 10254-10257.	13.7	18

#	Article	IF	CITATIONS
37	Dynamic Ca2+-Dependent Activity of Membrane-Anchored Synaptotagmin1 Observed at the Content Mixing Level. Biophysical Journal, 2013, 104, 89a.	0.5	0
38	Mechanical Unzipping and Rezipping of a Single SNARE Complex Reveals Large Hysteresis as the Force Generating Mechanism. Biophysical Journal, 2013, 104, 89a.	0.5	0
39	Mechanical unzipping and rezipping of a single SNARE complex reveals hysteresis as a force-generating mechanism. Nature Communications, 2013, 4, 1705.	12.8	96
40	Real-time single-molecule coimmunoprecipitation of weak protein-protein interactions. Nature Protocols, 2013, 8, 2045-2060.	12.0	31
41	Properties of Self-Quenching Fluorescence Dye for Vesicle-Vesicle Content Mixing System. Biophysical Journal, 2013, 104, 88a.	0.5	1
42	Simultaneous detection of biomolecular interactions and surface topography using photonic forcemicroscopy. Biosensors and Bioelectronics, 2013, 42, 106-111.	10.1	3
43	The synaptotagmin 1 linker may function as an electrostatic zipper that opens for docking but closes for fusion pore opening. Biochemical Journal, 2013, 456, 25-33.	3.7	26
44	Real-time single-molecule co-immunoprecipitation analyses reveal cancer-specific Ras signalling dynamics. Nature Communications, 2013, 4, 1505.	12.8	66
45	Simple super-resolution live-cell imaging based on diffusion-assisted Förster resonance energy transfer. Scientific Reports, 2013, 3, 1208.	3.3	50
46	In Situ Quantitative Imaging of Single-Molecule Co-Immunoprecipitation. Biophysical Journal, 2012, 102, 600a.	0.5	0
47	Direct Observation of Dual Pathways of Yeast Minimal-Machinery-SNARE Driven Vesicle Fusion. Biophysical Journal, 2012, 102, 499a.	0.5	0
48	Dynamic Ca2+-Dependent Activity of Membrane-Anchored Synaptotagmin 1 Observed at the Content Mixing Level. Biophysical Journal, 2012, 102, 502a.	0.5	0
49	Single Vesicle Fusion System for Content Mixing and SNARE Complex Formstion. Biophysical Journal, 2012, 102, 499a.	0.5	0
50	Quantification of Protein Concentration using Single Molecule Western Blot. Biophysical Journal, 2012, 102, 181a.	0.5	0
51	Observation of Two-Step Unzipping of a Single SNARE Complex by using Nano-Mechanical Measurement. Biophysical Journal, 2012, 102, 670a.	0.5	0
52	A single vesicle-vesicle fusion assay for in vitro studies of SNAREs and accessory proteins. Nature Protocols, 2012, 7, 921-934.	12.0	98
53	Efficient Single-Molecule Fluorescence Resonance Energy Transfer Analysis by Site-Specific Dual-Labeling of Protein Using an Unnatural Amino Acid. Analytical Chemistry, 2011, 83, 8849-8854.	6.5	27
54	Chasing the Trails of SNAREs and Lipids Along the Membrane Fusion Pathway. Current Topics in Membranes, 2011, 68, 161-184.	0.9	3

#	Article	IF	CITATIONS
55	Water Meniscus-Directed Organization of Liquid-Ordered Domains in Lipid Monolayer. Journal of Nanoscience and Nanotechnology, 2011, 11, 4527-4531.	0.9	5
56	MutS switches between two fundamentally distinct clamps during mismatch repair. Nature Structural and Molecular Biology, 2011, 18, 379-385.	8.2	120
57	Low-power nano-optical vortex trapping via plasmonic diabolo nanoantennas. Nature Communications, 2011, 2, 582.	12.8	108
58	Electrically Programmable Nematofluidics with a High Level of Selectivity in a Hierarchically Branched Architecture. ChemPhysChem, 2010, 11, 101-104.	2.1	19
59	Dynamic Ca ²⁺ -Dependent Stimulation of Vesicle Fusion by Membrane-Anchored Synaptotagmin 1. Science, 2010, 328, 760-763.	12.6	117
60	Dissection of SNARE-driven membrane fusion and neuroexocytosis by wedging small hydrophobic molecules into the SNARE zipper. Proceedings of the National Academy of Sciences of the United States of America, 2010, 107, 22145-22150.	7.1	47
61	Single-Vesicle Fusion Assay Reveals Munc18-1 Binding to the SNARE Core Is Sufficient for Stimulating Membrane Fusion. ACS Chemical Neuroscience, 2010, 1, 168-174.	3.5	43
62	Progress in understanding the neuronal SNARE function and its regulation. Cellular and Molecular Life Sciences, 2009, 66, 460-469.	5.4	17
63	C2AB: A Molecular Glue for Lipid Vesicles with a Negatively Charged Surface. Langmuir, 2009, 25, 7177-7180.	3.5	29
64	Complexin and Ca2+ stimulate SNARE-mediated membrane fusion. Nature Structural and Molecular Biology, 2008, 15, 707-713.	8.2	113
65	Topographic control of lipid-raft reconstitution in model membranes. Nature Materials, 2006, 5, 281-285.	27.5	79
66	Pixel-encapsulated flexible displays with a multifunctional elastomer substrate for self-aligning liquid crystals. Applied Physics Letters, 2006, 88, 263501.	3.3	29
67	Multiple intermediates in SNARE-induced membrane fusion. Proceedings of the National Academy of Sciences of the United States of America, 2006, 103, 19731-19736.	7.1	207
68	Patterning Process of Membrane-Associated Proteins on a Solid Support with Geometrical Grooves. Molecular Crystals and Liquid Crystals, 2005, 434, 297/[625]-303/[631].	0.9	2
69	UNDULATION PATTERNS IN PATTERN FORMATION OF CHOLESTERIC LIQUID CRYSTALS AS WAVELENGTH-CHANGING INSTABILITIES. Molecular Crystals and Liquid Crystals, 2004, 413, 489-497.	0.9	0
70	Spontaneous aggregation of lipids in supported membranes with geometrical barriers. Applied Surface Science, 2004, 238, 299-303.	6.1	3
71	Control of electric equi-potential in a liquid crystal film on a grating surface. Optical Materials, 2003, 21, 647-650.	3.6	0
72	A self-aligned multi-domain liquid-crystal display on polymer gratings in a vertically aligned configuration. Journal of the Society for Information Display, 2003, 11, 283.	2.1	5

#	Article	IF	CITATIONS
73	Multi-domain Liquid Crystal Display with Self-Aligned 4-Domains on Surface Relief Gratings of Photopolymer. Molecular Crystals and Liquid Crystals, 2002, 375, 433-440.	0.9	15
74	Self-formation of microdomains by the topographical and fringe field effects in a liquid crystal display with dielectric surface gratings. Applied Physics Letters, 2002, 81, 2361-2363.	3.3	6
75	P-91: Gray Scale Stabilization in a Twisted Nematic Liquid Crystal Display Mode on Self-Induced Micro-Domain Array. Digest of Technical Papers SID International Symposium, 2002, 33, 562.	0.3	Ο
76	Multi-domain Liquid Crystal Display with Self-Aligned 4-Domains on Surface Relief Gratings of Photopolymer. Molecular Crystals and Liquid Crystals, 2002, 375, 433-440.	0.3	2
77	Optical Properties of a Chiral Liquid Crystal in a Generalized Coupled Mode Formalism. Molecular Crystals and Liquid Crystals, 2001, 371, 203-206.	0.3	0
78	ANALYSIS OF THE OPTICAL PROPERTIES OF A HELICOIDAL LIQUID CRYSTAL IN A GENERAL COUPLED MODE FORMALISM. Molecular Crystals and Liquid Crystals, 2001, 366, 387-394.	0.3	0
79	Wavelength Selection in a Fabry-Perot Filter with an Axially Aligned Nematic Liquid Crystal. Molecular Crystals and Liquid Crystals, 1999, 337, 19-24.	0.3	1